

THE FLUXCOMPENSATOR: MAKING RADIATIVE TRANSFER MODELS OF HYDRODYNAMICAL SIMULATIONS DIRECTLY COMPARABLE TO REAL OBSERVATIONS

CHRISTINE M. KOEPFERL^{1,2} AND THOMAS P. ROBITAILLE^{1,3}

¹ Max Planck Institute for Astronomy, Königstuhl 17, D-69117 Heidelberg, Germany

² University Observatory Munich, Scheinerstr. 1, D-81679 Munich, Germany

³ Freelance Consultant, Headingley Enterprise and Arts Centre, Bennett Road Headingley, Leeds LS6 3HN

(Received 22nd June 2017; Accepted 14th August 2017)

The Astrophysical Journal

ABSTRACT

When modeling astronomical objects throughout the universe, it is important to correctly treat the limitations of the data, for instance finite resolution and sensitivity. In order to simulate these effects, and to make radiative transfer models directly comparable to real observations, we have developed an open-source Python package called the FLUXCOMPENSATOR that enables the post-processing of the output of 3-d Monte-Carlo radiative transfer codes, such as HYPERION. With the FLUXCOMPENSATOR, realistic synthetic observations can be generated by modeling the effects of convolution with arbitrary point-spread-functions (PSFs), transmission curves, finite pixel resolution, noise and reddening. Pipelines can be applied to compute synthetic observations that simulate observatories, such as the *Spitzer Space Telescope* or the *Herschel Space Observatory*. Additionally, this tool can read in existing observations (e.g. FITS format) and use the same settings for the synthetic observations. In this paper, we describe the package as well as present examples of such synthetic observations.

1. INTRODUCTION

Theoretical simulations (e.g. hydrodynamical simulations) are currently used to reproduce the physical processes in astronomical objects, such as young stellar objects (YSOs), star-forming regions and galaxies. However, we cannot use these simulations directly to predict or explain observational features of such objects. Instead, full radiative transfer calculations need to be performed to properly take into account effects, such as local temperature variations or changes in the optical depth. These radiative transfer calculations provide idealized observations, which are somewhat closer to real observations than the hydrodynamical simulations. In the last decade, the use of idealized observations, from radiative transfer techniques, has been made possible due to the development of full 3-d Monte-Carlo radiative transfer codes (see the extensive review of Steinacker et al. 2013). We list some publicly available examples below:

• RADMC3D

RADMC3D is a 3-d Monte-Carlo radiative transfer code (for details¹, see Dullemond & Dominik 2004). It can treat the dust radiative transfer but also gas line radiative transfer for local thermodynamical equilibrium (LTE) and non-LTE problems. It has a variety of different geometries implemented and is parallelized. It uses the modified random walk and raytracing.

• HYPERION

The 3-d dust continuum Monte-Carlo radiative transfer code HYPERION (for details², see Robitaille 2011), which is fully parallelized and is not dependent on specific synthetic astronomical ob-

jects but rather provides a generic set of geometries. HYPERION as other dust radiative transfer codes, treats all dust interactions, such as absorption, re-emission and scattering. HYPERION is an LTE code, and, in addition, can treat (simple) non-LTE approximations, such as the emission of polycyclic aromatic hydrocarbons (PAHs). It uses the Lucy method, the modified random walk, peeling-off and raytracing.

• MOCASSIN

MOCASSIN, a 3-d photoionization and dust non-LTE Monte-Carlo radiative transfer code (for details³, see Ercolano et al. 2003, 2005, 2008). The code is parallelized and contains a number of grid geometries.

• LIME

LIME is a molecular excitation and non-LTE spectral line radiation transfer code (for details⁴, see Brinch & Hogerheijde 2010) and contains different geometry set-ups and is fully parallelized.

• TORUS

p TORUS is a molecular line and photoionization code which makes use of the 3-d Monte-Carlo radiative transfer technique but also has hydrodynamics, radiation hydrodynamics and self-gravity built-in (for details⁵, see Harries 2000). It is fully parallelized, has different sets of geometry grids and uses the Lucy method.

Monte-Carlo radiative transfer codes (e.g. HYPERION) can read density structures from the output of theoretical simulations. At every grid point, they sample the

koepferl@usm.lmu.de

¹ <http://www.ita.uni-heidelberg.de/~dullemond/software/radmc-3d/>

² <http://www.hyperion-rt.org>

³ <http://mocassin.nebulousresearch.org>

⁴ <http://www.nbi.dk/~brinch/lime.php>

⁵ http://www.astro.ex.ac.uk/people/th2/torus_html/homepage.html

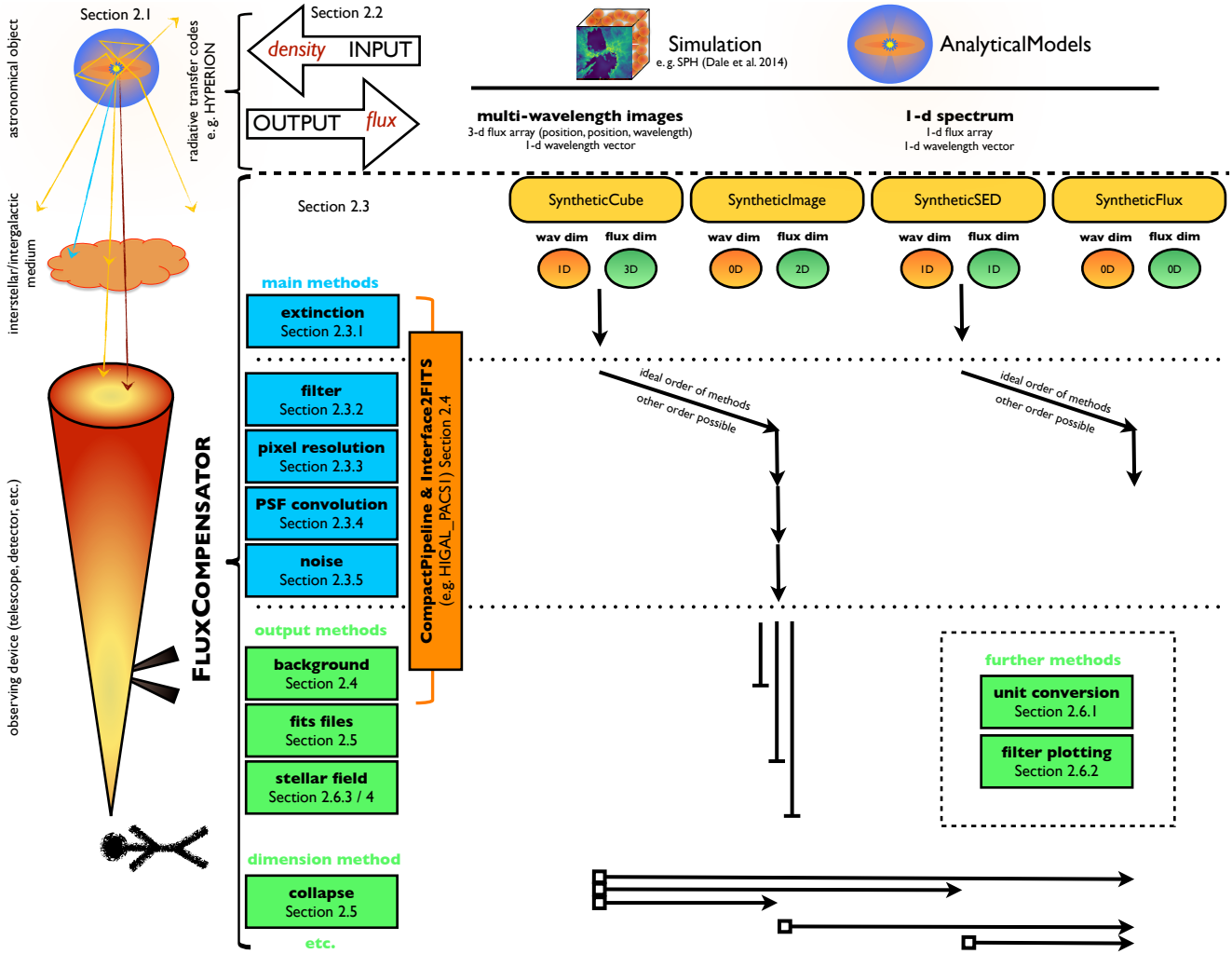


FIG. 1.— Flow scheme of the relevant HYPERION and FLUXCOMPENSATOR input/output structure and the analogy in reality. The relevant sections are highlighted within the scheme.

probability distributions of a photon being scattered, absorbed or re-emitted, which is propagating through the grid. As a result, the temperature is calculated and flux images can be generated in any given direction or wavelength. For more details, see Robitaille 2011 and the extensive review of Steinacker et al. 2013. The radiative transfer, however, only treats the ideal path of the photons from the astronomical object to the telescope. Concretely, with the mere solution of the radiative transfer problem the observational limitations of a telescope, such as finite resolution or the effects on the ideal synthetic observation by optics or detectors within the telescope, have so far not been accounted for. We, hereafter, call such synthetic observations (which lack the treatment of the observational effects) from radiative transfer calculation “ideal” synthetic observations.

We have developed a tool, called the FLUXCOMPENSATOR, which treats these limitations and produces “realistic” synthetic observations. Our tool links theoretical studies and radiative transfer modeling with actual astronomical observations by making them directly comparable. The tool was successfully applied in Koepferl et al. (2015), Ercolano et al. (2015) and Roccatagliata et al. (2015), as well as in the paper series “*Insights from Synthetic Star-forming Regions*” Koepferl et al.

(2016c,a,b) and the Milky Way Project⁶. In this paper, we now present the FLUXCOMPENSATOR tool, which produces these realistic synthetic observations from radiative transfer calculations. In Section 2, we describe the code and discuss its compatibility to other radiative transfer codes in Section 3. As an example in Section 4, we show realistic synthetic observations of a YSO model, a star-forming region and a center of a galaxy and discuss applications and future prospects for the code (Section 5), before summarizing the paper in Section 6.

2. CODE OVERVIEW

With the FLUXCOMPENSATOR (now available via <https://github.com/koepferl/FluxCompensator>, for scheme see Fig. 1) we can post-process radiative transfer calculations, such as from HYPERION (Robitaille 2011)⁷,

⁶ Citizen science project at zooniverse.org (Kendrew et al. 2016; Kerton et al. 2015; Beaumont et al. 2014; Kendrew et al. 2012; Simpson et al. 2012).

⁷ Note as the FLUXCOMPENSATOR was designed as an post-processing tool for HYPERION however it can be used by other codes. Therefore, the reader should see the HYPERION (Robitaille 2011) reference as an example of many other radiative transfer codes. For the remainder of this paper, however, we will use HYPERION as a place holder for other radiative transfer codes.

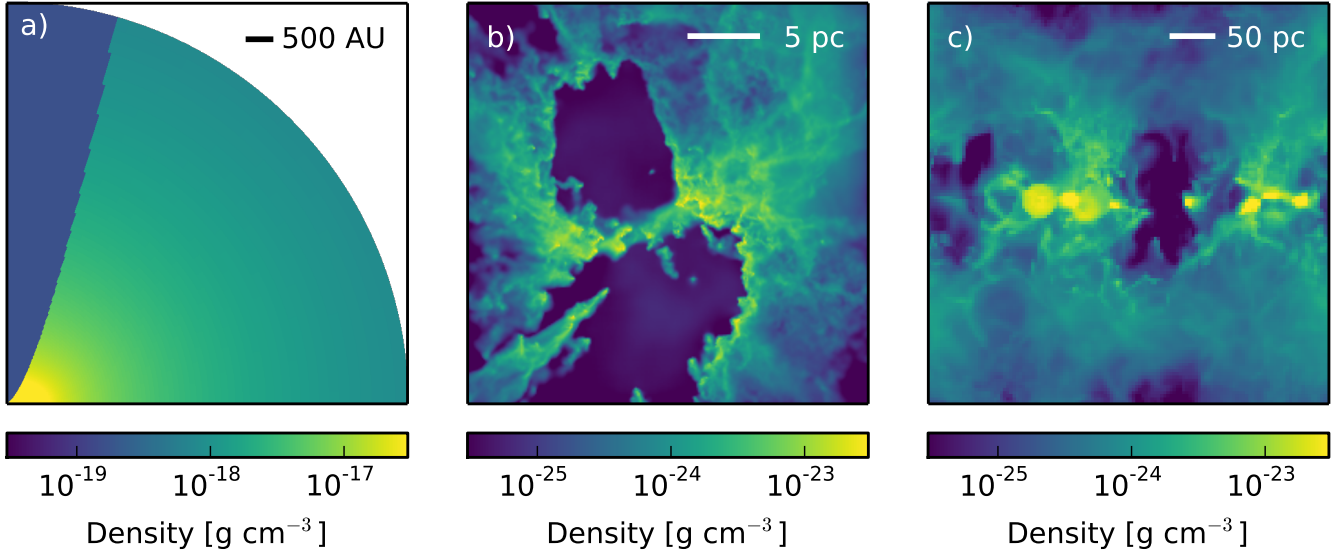


FIG. 2.— Total projected density of a) a YSO model, b) a star-forming region, and c) a center of a galaxy.

by reading in the radiative transfer output and using these, to produce realistic synthetic observations. The FLUXCOMPENSATOR follows the same philosophy as HYPERION in using object-oriented Python scripts and making it therefore more user friendly and generic. Very little Python knowledge is required to work with either HYPERION or the FLUXCOMPENSATOR. For the compatibility with other radiative transfer codes see Section 3.

For the comprehension of the following sections Figure 1 is helpful where we visualized the methodology of the FLUXCOMPENSATOR and the concept of synthetic observation in a flow scheme. The relevant sections are highlighted within the scheme.

2.1. Life of a Real Photon

In nature, photons emitted from a source are scattered, absorbed and re-emitted by matter (dust and gas) in astronomical objects (e.g. YSOs, star-forming regions, galaxies). These photon processes happen many times as they propagate through matter. Absorption of photons by dust and gas causes the matter to heat up. The emitted light from the astronomical object (in form of photons) is reddened by interstellar extinction. Further only some of the emitted photons reach the telescope, because of its finite opening angle. Photons of different energy enter the telescope. The beam of light diffracts at the opening of the telescope. The diffraction pattern is described by the PSF of the telescope⁸. The spectral transmission⁹ of the telescope further filters the radia-

⁸ In a non-ideal observational system also atmospheric matter (e.g. seeing) which causes the PSF to blur. For space observatories no seeing exists while the shapes of the PSFs depend merely on the characteristics of the instruments. The angular resolution of the telescope with diameter D relates to λ/D . Note that the above is strictly only true infrared light or shorter wavelengths not for the radio emission, where the distortion is called beam and can no longer be approximated by an Airy disc.

⁹ Note that when we speak of spectral transmission of the "telescope and detector" we refer to all effects introduced by parts of the observing device (e.g. filters, telescope configuration, dispersive elements) that select wavelength specific photons. This filtering introduces flux loss, also in the non-selected wavelength areas of the

tion in such a way that only photons within a certain wavelength range can reach the detector.

The light of the photons detected can either be measured by a single value – the photometric flux which is a scalar – or by spatially resolving the light – photometric images, which are essentially 2-d flux arrays. If we measure photometric fluxes for different filters, instruments, or telescopes, these can then be combined into 1-d spectrum¹⁰. Observational images are produced by exposing many pixels in a two-dimensional configuration to the photons. The pixels map the projected positions, of the last location where the photons interacted in the observed object, onto a 2-d plane¹¹. The images are also altered by the PSF of the telescope and furthermore, the pixel resolution of the detector has an important effect on the images.

2.2. Life of a Synthetic Photon in HYPERION

HYPERION is a 3-d dust continuum Monte-Carlo radiative transfer tool that can take any arbitrary 3-d distribution of dust and sources, and compute the temperature structure as well as idealized multi-wavelength observations.

It can be used to compute ANALYTICALMODELS (toy models with an analytical density distribution), such as YSOs (see Figure 2(a)), but it can also read in any arbitrary 3-d density distributions from hydrodynamical simulations (see Figure 2(b,c)). Figure 2(b) shows a time-step in a smooth particle hydrodynamics (SPH) simulation of a $10^4 M_\odot$ star-forming region by Dale et al. (2012). In this particular run only ionizing sources contribute to the stellar feedback. In Figure 2(c), we see the surface density of a center of a galaxy extracted from the simulations performed by the SILCC collaboration (Girichidis et al. 2016; Walch et al. 2015).

spectrum. Only when the "spectral transmission function" is not a normalized box function the flux loss in the selected wavelength range is zero.

¹⁰ 1-d flux and wavelength vector

¹¹ 2-d flux array (position, position) and scalar wavelength

TABLE 1
CLASS DIMENSIONS IN THE FLUXCOMPENSATOR

class	flux	wavelength
SyntheticCube	3-d (x, y, wav)	1-d array
SyntheticImage	2-d (x, y)	0-d array
SyntheticSED	1-d (wav)	1-d array
SyntheticFlux	0-d (wav)	0-d array

HYPERION samples probability distribution functions (PDFs) for the photon interactions and computes the temperatures in the grid. The photons interact with the dust and eventually can escape the system. The photons escaping in the direction of the telescope are then used to produce the synthetic observations. Depending on the initial set-up, 1-d spectrum¹⁰ and/or multi-wavelength images¹² are produced. HYPERION scales these ideal synthetic observations to a certain distance and converts these to the requested units once they are extracted. For more details see Robitaille (2011).

2.3. Virtual Pipeline of the FLUXCOMPENSATOR

The FLUXCOMPENSATOR uses 3-d spectral cubes¹² or 1-d spectrum¹⁰ from radiative transfer calculations and simulates the effects which are introduced by the telescope. In order to make the FLUXCOMPENSATOR user-friendly, the framework itself can support any transmission curve and PSF file provided by the user. Furthermore, we have included common extinction laws, PSF files, spectral transmission curves and further information in the database of the FLUXCOMPENSATOR. For references and the extent of the information in the database, see Table 2 in Appendix A. It is left up to the users whether they use this database or whether they just use the methods of the FLUXCOMPENSATOR but load their preferred resources with a separate line of code instead.

The dimensions of the observations in flux change when passing through the telescope and the detectors. For example, multi-wavelength photons that enter the telescope can be represented by an idealized 3-d spectral cube. The spectral transmission of the telescope and detector, filters only photons within certain slices of this spectral cube and weights them, so that a two-dimensional image remains. The FLUXCOMPENSATOR therefore has four different classes to treat the different dimensions: **SyntheticCube**, **SyntheticImage**, **SyntheticSED**, **SyntheticFlux**. Each has a different flux and wavelength dimension, as highlighted in Table 1. The methods of the FLUXCOMPENSATOR can be called in any arbitrary order as long as the dimensions allow it (i. e. one cannot apply a filter transmission curve to a 2-d image). The order might affect the speed of the numerical calculation, while producing a comparable physical result. In the following sections, we will present one scenario of using the methods of the FLUXCOMPENSATOR which simulates the effects, such as those introduced by a telescope and its detector. Pipelines with a different order of the methods (e. g. extinction, PSF convolution,

noise) presented in Sections 2.3.1 to Sections 2.3.5 are also supported. Not all methods need to be applied and the user can select those appropriate for the specific scientific question.

From Section 2.3.1 to Section 2.3.5, we will illustrate the transformation within the pipeline of the synthetic observations from ideal to realistic, by using snapshots displayed in Figure 3. Figure 3(a) shows the ideal synthetic observation slice extracted from the HYPERION output closest to 70 μm .

2.3.1. Extinction

The photons emitted from the astronomical objects do not usually reach the observing telescope unaffected by extinction (between the object and telescope). By accounting for interstellar reddening (see Carroll & Ostlie 2014, 1996) the observations are made more realistic. The FLUXCOMPENSATOR supports loading arbitrary extinction laws (or provides the law¹³ of Kim et al. 1994 in the database).

With the opacity values k_λ provided by the extinction law, we can estimate the wavelength-dependent extinction A_λ with

$$A_\lambda = A_V \cdot \frac{k_\lambda}{k_V}, \quad (1)$$

where the optical extinction A_V is a free input parameter, k_V is interpolated by the FLUXCOMPENSATOR from k_λ at optical wavelengths with linear interpolation (see Press et al. 1992). We redden the flux with

$$F_{\text{extincted}}(\lambda) = F_{\text{intrinsic}}(\lambda) \cdot 10^{-0.4 \cdot A_\lambda}. \quad (2)$$

We show the reddened Figure 3(b) Photoconductor Array Camera and Spectrometer (PACS) 70 μm synthetic image in Figure 3(c). We used the extinction law from the FLUXCOMPENSATOR database and assumed an optical extinction of $A_V = 500$. At 70 μm , the effect of extinction is negligible. Therefore, realistic values e. g. $A_V = 20$, would make Figure 3(c) indistinguishable from Figure 3(b). For now, for illustration purposes we adapt this "unphysical" value.

Note that the reddening of the observation is due to interstellar or intergalactic extinction and is not strictly an instrumental effect as remaining effects which can be simulated with the FLUXCOMPENSATOR.

2.3.2. Spectral Transmission Convolution

When photons of different energies pass through a detector in a real telescope, their different energies (or wavelengths) are weighted by the transmission of the whole system – optics, filter, camera (see Carroll & Ostlie 2014, 1996). In the FLUXCOMPENSATOR an algorithm performs the rebinning of the spectral transmission and the convolution with the multi-wavelength images or 1-d spectrum. The resulting 2-d **SyntheticImage** (of an initial 3-d **SyntheticCube**) or a 0-d **SyntheticFlux** (of an initial 1-d **SyntheticSED**) represent the flux observed by the detector.

The tool can either load arbitrary transmission curves with an extra line of code or use the transmission curves from the database. In Figure 3(b), we present

¹² 3-d flux array (position, position, wavelength) and 1-d wavelength vector

¹³ Note that this extinction law breaks down above 1 mm.

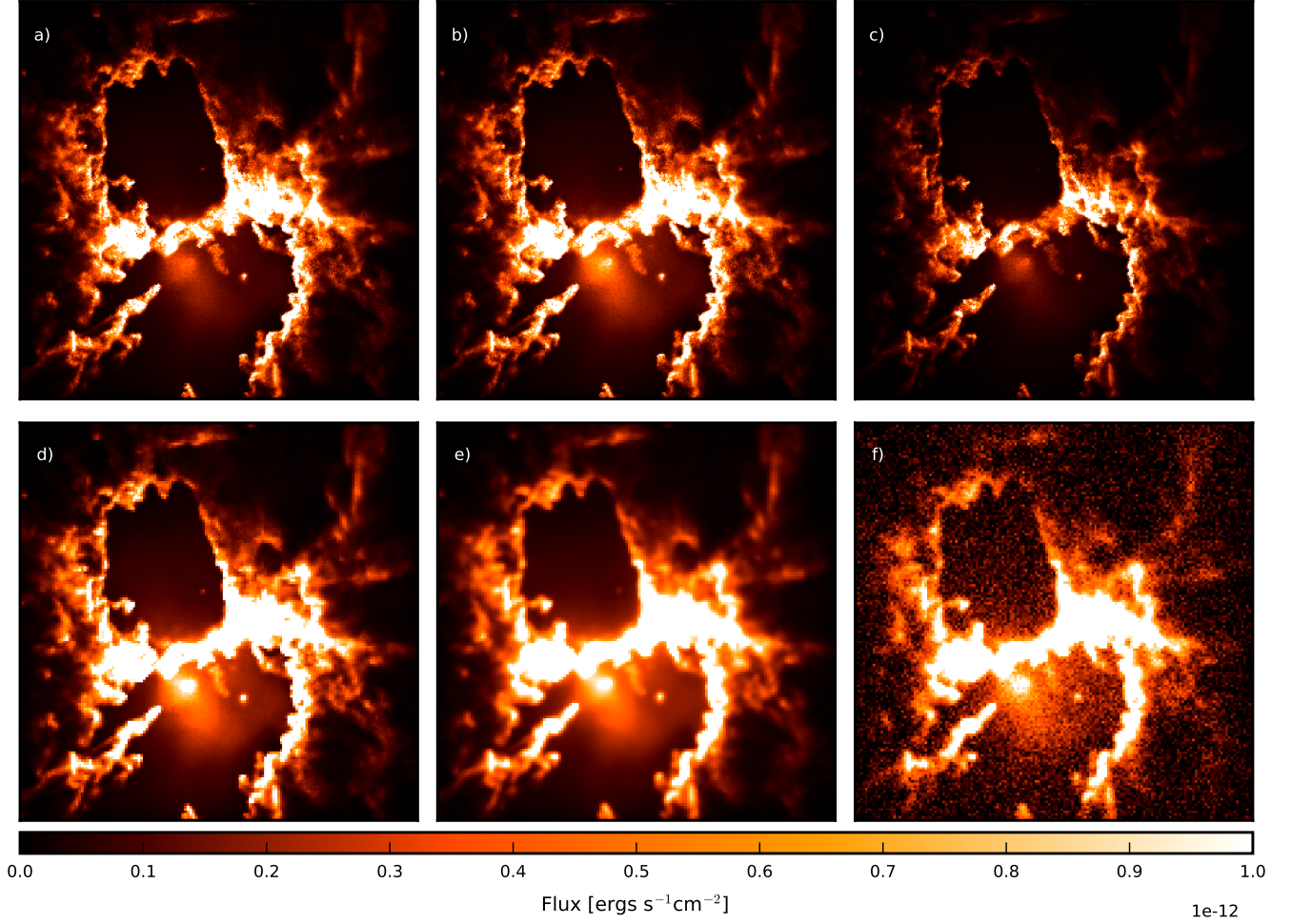


FIG. 3.— Snapshots during the ongoing pipeline: a) HYPERION output image slice closest to $\lambda = 70 \mu\text{m}$, b) image after convolution with PACS $70 \mu\text{m}$ transmission curve, c) PACS $70 \mu\text{m}$ image after reddening, d) PACS $70 \mu\text{m}$ image with corresponding pixel resolution, e) PACS $70 \mu\text{m}$ image after PACS PSF convolution, f) PACS $70 \mu\text{m}$ with Gaussian noise.

the synthetic image, where Figure 3(a) was weighted with a PACS $70 \mu\text{m}$ filter from the FLUXCOMPENSATOR database. The database currently has 24 transmission curves from Two Micron All-Sky Survey (2MASS), *Spitzer*, *Herschel*, Infrared Astronomical Satellite (IRAS) and Wide-field Infrared Survey Explorer (WISE) with central wavelengths from $1.235 \mu\text{m}$ to $500 \mu\text{m}$. Table 2 in Appendix A lists the information about the filter transmissions and their references.

For arbitrary loaded filters, two parameters are passed to the FLUXCOMPENSATOR which represent the nature of the filter (Robitaille et al. 2007). The first parameter is α , which resembles the taken assumptions in order to convert the flux into the monochromatic flux density F_ν :

$$\nu^\alpha F_\nu = \text{const.} \quad (3)$$

The transmission in a filter curve file $R_{\nu,\text{input}}$ goes such as

$$R_{\nu,\text{input}} = R_\nu \nu^\beta \quad (4)$$

to the filter transmission R_ν . The units of the transmission curve are set by the exponent β . When the transmission curve is given as a function of photons $\beta = 0$, while $\beta = -1$ when the transmission is given as a func-

tion of energy. See Table 2 in Appendix A for α and β values of the filters in the database and their references.

To weight the synthetic data with the spectral transmission, the FLUXCOMPENSATOR calculates the effective spectral response (Robitaille et al. 2007) at every wavelength slice of the 3-d SyntheticCube or 1-d SyntheticSED:

$$R_{\nu,\text{response}} = \frac{1}{\nu_0^\alpha} \frac{R_{\nu,\text{input}}/\nu^{1+\beta}}{\int R_{\nu,\text{input}}/\nu^{1+\alpha+\beta}}, \quad (5)$$

where ν_0 is the central frequency of the filter. The sum of the weighted flux with the spectral response then gives the filtered flux:

$$F_{\nu_0,\text{filtered}} = \sum_{\nu=\nu_{\min}}^{\nu_{\max}} R_{\nu,\text{response}} F_\nu, \quad (6)$$

within the limits of the filter ν_{\min} and ν_{\max} . For more details see the Appendix of Robitaille et al. (2007).

2.3.3. Pixel Resolution

The pixel resolution of the initial ideal synthetic observation is determined by the set-up of the radiative transfer model and by the distance, which is set by the

user in the HYPERION model. The resulting pixel resolution remains constant until actively changed. From Figure 3(a) to Figure 3(c) the images are still in the intrinsic resolution of about $2''$.

However, with the FLUXCOMPENSATOR, the user can also change the pixel resolution after the radiative transfer calculation. This might be useful for example to compare the synthetic observations with a real observation from a certain detector with a specific pixel resolution. This is especially necessary if PSF convolution with a telescope-specific PSF file is anticipated.

We have designed an algorithm which redistributes the flux from the initial pixels (within `SyntheticCube` and `SyntheticImage`) to a new grid of different size and which causes a change in pixel resolution. Its efficiency is of $\mathcal{O}(N^2)$ and is flux and brightness conserving.

In Figure 3(d), the synthetic image of Figure 3(c) was rescaled to a pixel resolution of $4''$, which is a specific pixel resolution used for PACS 70 μm images.

2.3.4. PSF Convolution

The effects of diffraction (see Carroll & Ostlie 2014, 1996; Feynman 1977) at the opening of the observing telescope represent one of the largest effects which distinguishes real from ideal observations¹⁴. The FLUXCOMPENSATOR supports currently three different approaches of convolving (see Bronstein et al. 2005; Press et al. 1992) an image (within `SyntheticCube` and `SyntheticImage`) with a PSF:

- PSF File

It is a good choice to convolve the image with a PSF file which was provided in the telescope’s documentation. Any arbitrary PSF file is supported and can be easily added (with one additional line of code) and a `FilePSF` object can be constructed. Instances of the `FilePSF` class for the *Spitzer Space Telescope* and *Herschel Space Observatory* are already stored in the database of the FLUXCOMPENSATOR. In Figure 3(e), the synthetic image of Figure 3(d) was convolved with the PACS 70 μm `FilePSF` class provided in the database. Currently, the database has 28 `FilePSF` classes constructed by PSF files from *Spitzer* (Infrared Array Camera (IRAC), Multiband Imaging Photometer for *Spitzer* (MIPS)) and *Herschel* (PACS, Spectral and Photometric Imaging Receiver (SPIRE)). They were obtained from the documentation for the various telescopes (for references see Table 2 in Appendix A).

- Gaussian

Diffraction at a circular opening of an optical or infrared telescope with diameter d is mathematically expressed by a PSF profile which is an Airy function (see Carroll & Ostlie 2014, 1996). To a first order approximation this profile can be represented by a 2-d Gaussian. For an image with pixel resolution θ in radians per pixel, the standard deviation σ_{Gauss} of the Gaussian profile (see Bronstein et al.

2005) is given by

$$\sigma_{\text{Gauss}} = \frac{1}{2\sqrt{2\ln 2}} \frac{\lambda}{d\theta} \quad (7)$$

in units of pixels. The class `GaussianPSF` within the FLUXCOMPENSATOR then sets up this PSF and a method convolves the image with this Gaussian profile.

- Arbitrary Function

In some cases it might be reasonable to convolve the image with an array constructed from an arbitrary function. The FLUXCOMPENSATOR supports this with the class `FunctionPSF`.

In any case, it is important to adjust the pixel resolution to the observing detector’s pixel resolution before convolving with any PSF class described above (see Section 2.3.3). Further caution is necessary if the class `FilePSF` is applied on `SyntheticCube`. A single PSF may not be applicable to all wavelengths in the spectral cube. Therefore, we recommend to first convolve with a filter (see Section 2.3.2) and then convolve with `FilePSF`, which is also numerically faster. In future we may implement a wavelength-dependent PSF.

2.3.5. Noise

While observing, the statistical noise in an image depends on properties, such as the exposure time and/or the noise contribution from the reading of the camera grid (Howell 2006).

The FLUXCOMPENSATOR provides a random Gaussian noise method, which adds noise to the images (images in `SyntheticCube` and `SyntheticImage`). The input values are the mean μ_{noise} and the standard deviation σ_{noise} (in the units of the image) of the Gaussian random distribution (see Press et al. 1992).

It is possible that in future the FLUXCOMPENSATOR will be able to estimate the standard deviation directly from the information provided about the specific detector in the built-in database. In Figure 3(f), a noise of level $\sigma_{\text{noise}} = 7 \times 10^{-14} \text{ ergs s}^{-1} \text{ cm}^{-2}$ has been assumed for illustration purposes.

2.3.6. Example Pipeline

In the following, we give an example of what a virtual pipeline looks like: We load the Python modules (line 1 to 5), read in the HYPERION output (line 7 to 8), start the FLUXCOMPENSATOR (line 10 to 11), account for filter convolution (line 13 to 18), extinction (line 20 to 21), pixel resolution (line 23 to 24), PSF convolution (line 26 to 31) and noise (line 33 to 34).

```

1 import numpy as np
2
3 from hyperion.model import ModelOutput
4 from hyperion.util.constants import pc, kpc
5 from fluxcompensator.cube import *
6
7 m = ModelOutput('hyperion_output.rtout')
8 rt_model = m.get_image(group=0, inclination=0,
9                        distance=10 * kpc,
10                       units='ergs/cm^2/s')
11
12 # initial SyntheticObservation array
13 c = SyntheticCube(input_array=rt_model,
14                  unit_out='ergs/cm^2/s',
```

¹⁴ Note that this strictly only effects infrared and shorter wavelengths not the radio emission.

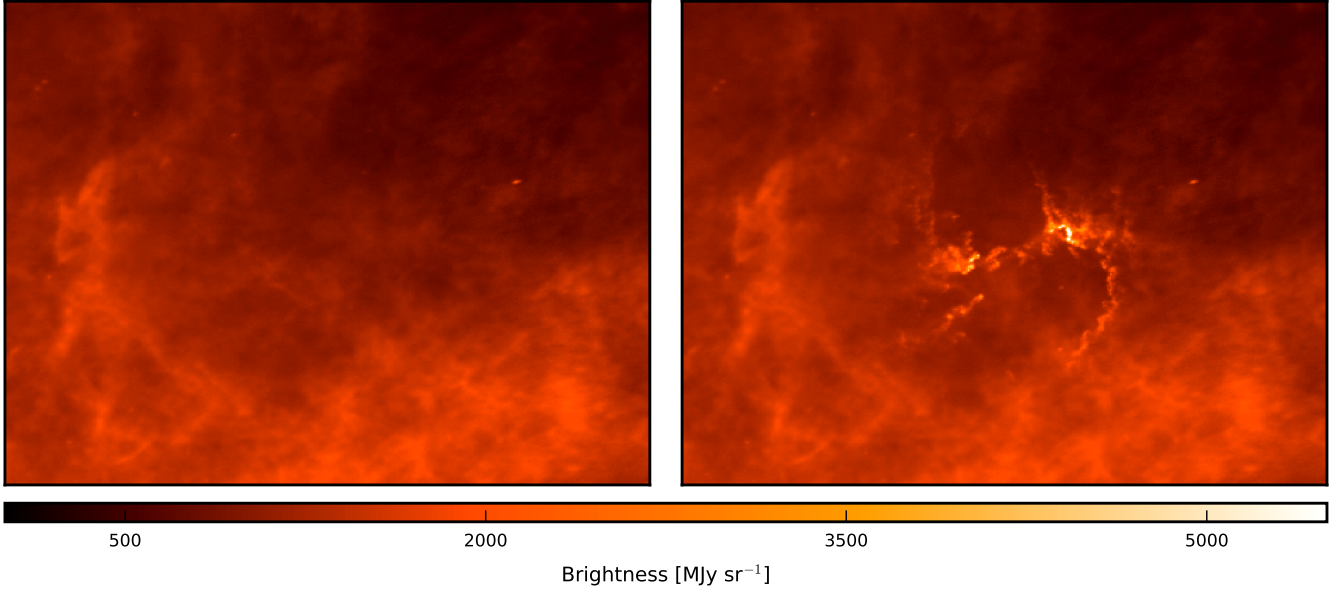


FIG. 4.— Before/after visualization of the realistic synthetic observation (right) of a star-forming region added to a PACS 70 μm *Herschel* Infrared Galactic Plane Survey (Hi-GAL) observation (left/right).

```

15         name='test_cube')
16
17 # call object from the filter database
18 import fluxcompensator.database.missions as filters
19 filter_input = filters.PACS1_FILTER
20
21 # convolve with filter
22 filtered = c.convolve_filter(filter_input)
23
24 # dered with provided extinction law
25 ext = filtered.extinction(A_v=20.)
26
27 # change pixel resolution to
28 # PACS1 pixel resolution
29 zoom = ext.change_resolution(
30     new_resolution=
31     filters.PACS1_PSF_RESOLUTION)
32
33 # call object from the psf database
34 import fluxcompensator.database.missions as PSFs
35 psf_object = PSFs.PACS1_PSF
36
37 # convolve with PSF
38 psf = zoom.convolve_psf(psf_object)
39
40 # add noise
41 noise = psf.add_noise(mu_noise=0,
42                       sigma_noise=7e-14)

```

In 42 lines of code we have shown how to create a realistic synthetic observation (here in PACS 70 μm).

2.4. Compact Pipelines and Synthetic Interface to Observation Files

Since the FLUXCOMPENSATOR (now available via <https://github.com/koepferl/FluxCompensator>) is constructed as an Python module, it is possible to construct and loop over entire pipelines, such as the example of Section 2.3.6, and to generate realistic synthetic images for different detectors and telescopes. The feature `CompactPipeline` in the FLUXCOMPENSATOR can be used to construct a wrapping code around an existing pipeline.

`CompactPipeline` can pass a mixture of self-constructed PSF or Filter classes and/or usage of the

database and classes such as `GaussianPSF`. The FLUXCOMPENSATOR supports the construction of these compact pipelines but also provides pre-constructed compact pipelines of the major infrared continuum surveys 2MASS, Galactic Legacy Infrared Mid-Plane Survey Extraordinaire (GLIMPSE), WISE, MIPS Galactic Plane Survey (MIPSGAL), Hi-GAL:

- 2MASS: `TWOMASSSURVEY_J`, `TWOMASSSURVEY_H`, `TWOMASSSURVEY_K`
- GLIMPSE: `GLIMPSE_IRAC1`, `GLIMPSE_IRAC2`, `GLIMPSE_IRAC3`, `GLIMPSE_IRAC4`
- MIPSGAL: `MIPSGAL_MIPS1`, `GLIMPSE_MIPS2`
- WISE: `WISESURVEY_WISE1`, `WISESURVEY_WISE2`, `WISESURVEY_WISE3`, `WISESURVEY_WISE4`
- Hi-GAL: `HIGAL_PACS1`, `HIGAL_PACS3`, `HIGAL_SPIRE1`, `HIGAL_SPIRE2`, `HIGAL_SPIRE3`

Further, the synthetic interface class, called `Interface2FITS`, acts as an interface between observations (e.g., Flexible Image Transport System – or FITS – files) and the ideal radiative transfer output. It supports the direct comparison of real observations stored in FITS files. The FLUXCOMPENSATOR reads information from the header of the FITS file in order to produce realistic synthetic observations with the same wavelength, reddening, pixel resolution and PSF specific for telescope and detector of the real observation. Information, such as the distance, the optical extinction coefficient of the object and the exposure time and/or noise contribution, are input parameters. It is also possible to load detector and telescope information which are not available in the built-in database.

When using the built-in interface little knowledge of Python programming is required. We show an example of the FLUXCOMPENSATOR interface code: the Numpy (van der Walt et al. 2011), FLUXCOMPENSATOR and HYPERION modules are loaded (line 1 to 5); the radiative

transfer spectral cube is read in (line 7 to 8); the realistic synthetic observation is produced and saved to a FITS file (line 10 to 12). It is further possible to combine the realistic synthetic observation with the original FITS file of the real observation at a given location (line 13). When comparing the synthetic observation directly with an astronomical object the `Interface2FITS` might be helpful since it replaces the background estimation.

```

1 import numpy as np
2 from hyperion.model import ModelOutput
3 from hyperion.util.constants import kpc
4 from fluxcompensator.interface import Interface2FITS
5 from fluxcompensator.database.pipeline import HIGAL_PACS1
6
7 m = ModelOutput('hyperion_output.rtout')
8 rt_model = m.get_image(group=0, inclination=0,
9                        distance=10*kpc,
10                       units='ergs/cm^2/s')
11
12 fluxcompensator = Interface2FITS(
13     obs='real_obs_pacs70.FITS',
14     model=rt_model,
15     pipeline=HIGAL_PACS1,
16     exposure=10,
17     A_v=20)
18
19 fluxcompensator.save2FITS('synthetic_obs')
20 fluxcompensator.add2observation('add2obs',
21                               position_pix=(3000,2500))

```

In Figure 4, we see the output of this code when starting with the radiative transfer model constructed from the density distribution provided by SPH simulations of Dale et al. (2012). Compare this result with Figure 2(b) and note how well this synthetic star-forming region blends into the Hi-GAL (Molinari et al. 2010) background.

2.5. Pipeline Post-processing & Outputs

When starting from a 3-d scalar cube from HYPERION, it might be interesting to inspect the current spectral energy distribution (SED) at some steps in the pipeline. With the FLUXCOMPENSATOR, it is possible at every step in the pipeline to convert a 3-d spectral cube (`SyntheticCube`) to a rough SED (`SyntheticSED`). Additionally, the FLUXCOMPENSATOR provides an algorithm to extract a photometric flux within wavelength bins from the 3-d spectral cube (`SyntheticCube`). The resulting object resembles a `SyntheticFlux`, but obtained without filter convolution. Furthermore, during the pipeline one can extract also the flux within certain wavelength bins: the resulting object is a `SyntheticFlux` object. Furthermore, for the object `SyntheticImage` the total fluxes can be extracted any time.

The FLUXCOMPENSATOR can produce a variety of outputs. With one line of Python code, users can output the resulting image to a FITS file, a pre-formatted plot or one can plot SEDs and photometric fluxes together. This can be done at any stage of the pipeline and also when synthetic interfaces are used.

It is also possible to create multi-color images or movies of different inclinations or time-steps as it was already possible for the HYPERION outputs. For further information visit <http://www.hyperion-rt.org> or <https://github.com/koepferl/FluxCompensator> and <http://FluxCompensator.readthedocs.io>.

2.6. Further Features

Additional tools and features are provided by the FLUXCOMPENSATOR and are described below:

2.6.1. Unit Conversion

The FLUXCOMPENSATOR can convert fluxes, flux densities and surface brightnesses (see Section 2.3) between the following units:

- $\text{ergs s}^{-1} \text{cm}^{-2}$
- $\text{ergs s}^{-1} \text{cm}^{-2} \text{Hz}^{-1}$
- Jy
- mJy
- MJy sr^{-1}
- Jy arcsec^{-2}

It is further possible for scalar fluxes (e.g. as member of `SyntheticFlux`) to convert to magnitudes. For the filters in the database we list the required zero-magnitude flux. Otherwise this information should be specified by the user. For the zero-magnitude flux of the detectors included in the built-in database and their references, see Table 2 in Appendix A.

2.6.2. Spectral Transmission Curve Visualization

The FLUXCOMPENSATOR provides a plotting tool to visualize the spectral transmission functions of chosen filters from the database and/or input filter curves. It is possible to compare transmission curves with different axis scaling and units.

2.6.3. Stellar Field

For a given 2-d image (`SyntheticImage`) the FLUXCOMPENSATOR can add a given number of foreground and background stars to the image and can deal with the extinction by the density distribution in the model (for the background stars) and PSF convolution effects. For an illustration of this, see Figure 5. To create a realistic stellar field, this feature of the FLUXCOMPENSATOR can be used in combination with stellar population synthesis models (e.g. Robin et al. 2003).

3. COMPATIBILITY WITH OTHER CODES

The FLUXCOMPENSATOR package has been designed to be able to post-process the radiative transfer output of HYPERION. It follows the same philosophy as HYPERION in using object-oriented Python scripts and making it therefore more user friendly and generic. Very little Python knowledge is required to work with either HYPERION or the FLUXCOMPENSATOR. As the tool has been designed for HYPERION, some features of the FLUXCOMPENSATOR will only work optimally if HYPERION inputs are used. However, in principle it should be easy to adapt the FLUXCOMPENSATOR so that it can read in any arbitrary ideal observations from other radiative transfer codes (e.g. those listed in Section 1), provided that they can output a spectral cube. Aside from the input, most of the code is not specific to HYPERION.

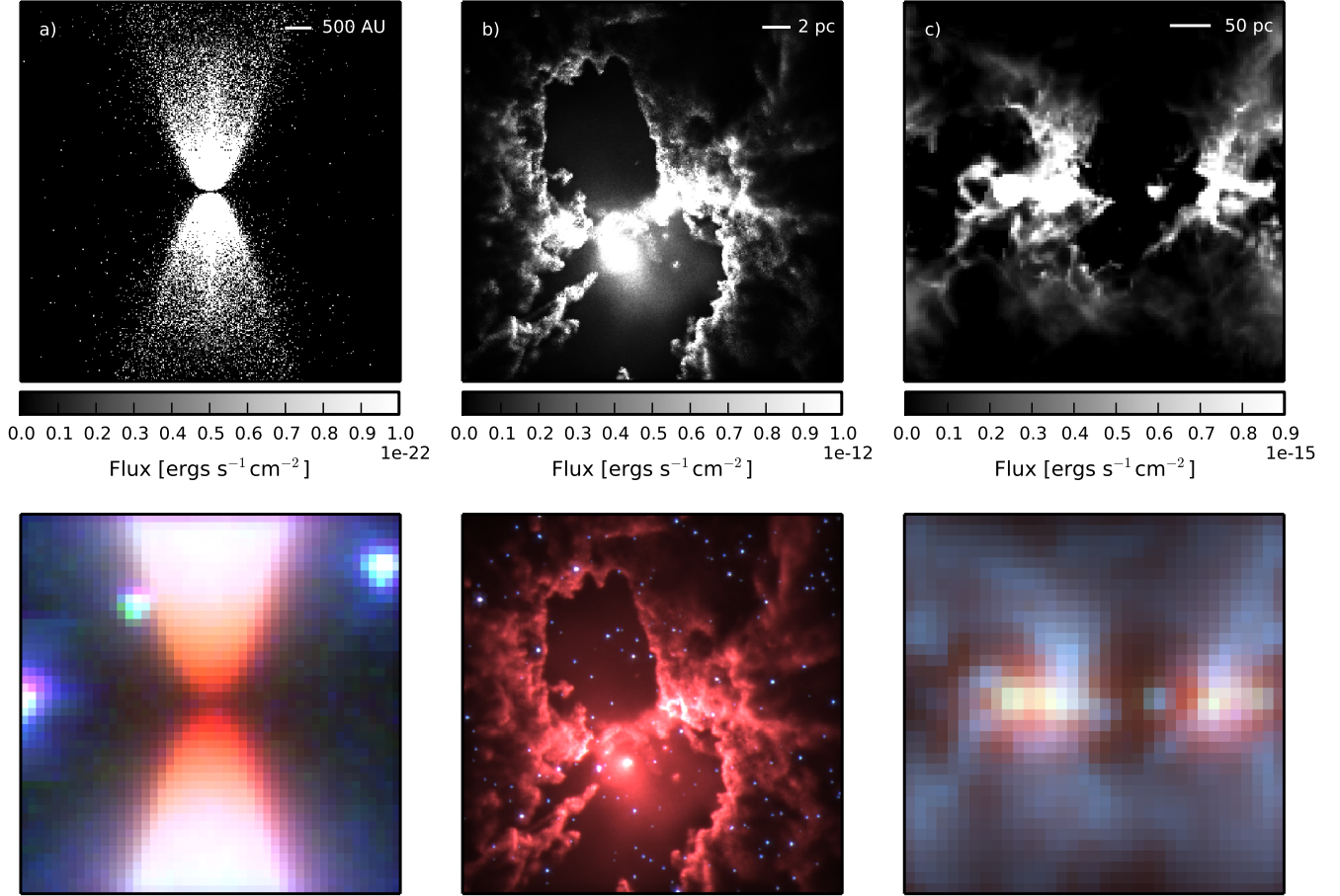


FIG. 5.— In column a) a YSO model at 140 pc, b) a star-forming region at 10 kpc and c) the center of a galaxy at 500 kpc. Top: Ideal single band synthetic observation at about 8 μm (a, b) and at about 500 μm (c) extracted directly from the radiative transfer output. Bottom: a,b) Realistic synthetic three-color images including field stars in GLIMPSE colors and c) *Herschel* three-color image. The maximum value of the stretch for the fluxes in IRAC 8 μm , IRAC 4.5 μm , IRAC 3.6 μm (RGB) are $3.0 \times 10^{-14} \text{ ergs s}^{-1} \text{ cm}^{-2}$ (red), $4.2 \times 10^{-14} \text{ ergs s}^{-1} \text{ cm}^{-2}$ (green) and $1.3 \times 10^{-14} \text{ ergs s}^{-1} \text{ cm}^{-2}$ (blue) for Figure 5(a) and $1.2 \times 10^{-13} \text{ ergs s}^{-1} \text{ cm}^{-2}$ (red), $2.0 \times 10^{-13} \text{ ergs s}^{-1} \text{ cm}^{-2}$ (green) and $8.0 \times 10^{-14} \text{ ergs s}^{-1} \text{ cm}^{-2}$ (blue) for Figure 5(b). The maximum value of the stretch for the fluxes in SPIRE 500 μm , PACS 160 μm , PACS 70 μm (RGB) in for Figure 5(c) are $3.0 \times 10^{-14} \text{ ergs s}^{-1} \text{ cm}^{-2}$ (red), $2.8 \times 10^{-13} \text{ ergs s}^{-1} \text{ cm}^{-2}$ (green) and $9.3 \times 10^{-15} \text{ ergs s}^{-1} \text{ cm}^{-2}$ (blue).

4. POSSIBLE APPLICATIONS

We show additional features of the FLUXCOMPENSATOR in this section and produce realistic synthetic observations of a YSO model, a star-forming region and a center of a galaxy. This time we will not combine the realistic synthetic observation with a real observation as was done in Figure 4. We rather produce three color images and additionally use the stellar field option to include reddened field stars to make them even more realistic.

In the case of the YSO, we used the built-in YSO toy model setup in HYPERION to construct the density distribution (see Figure 2(a)). For the star-forming region we used the density distribution displayed in Figure 2(b), which was calculated from hydrodynamical simulations by Dale et al. (2012). For the edge-on view of a center of a galaxy we used the dust temperature including gas-to-dust heating effects, which was calculated within the SILCC collaboration (Girichidis et al. 2016; Walch et al. 2015), to produce synthetic observations. The density distribution of the galaxy is shown in Figure 2(c).

With the FLUXCOMPENSATOR, we extract three-color

images in the colors of the GLIMPSE survey displayed in Figure 5(a,b). The ideal synthetic observations (at about 8 μm) of the realistic synthetic observations are also plotted in Figure 5(a,b). For the central region of a galaxy we show a three-color Hi-GAL image in Figure 5(c). In this case, field stars are not added. We plot the ideal synthetic observation (at about 500 μm) from HYPERION.

Realistic synthetic observations (as in Figure 3, Figure 4 and Figure 5) can help to critically test tools used by observers (e.g. structure finding mechanisms, modified blackbody fitting) to extract physical quantities (e.g. star-formation rates (SFRs), gas masses) from real observations.

In Koepferl et al. (2015) we found that the SFR in the central molecular zone (CMZ) of the Milky Way was overestimated by at least a factor of 3 by Yusef-Zadeh et al. (2009), who derived the SFR directly from YSOs detected at 24 μm . Aided by the FLUXCOMPENSATOR in Koepferl et al. (2015) we showed that the misclassified YSOs, which lead to the overestimation of the rate,

could also be main-sequence stars or other more evolved objects in an ambient medium. We provided classification criteria which will help in future when classifying YSOs in this region.

In Koepferl et al. (2016c) we went one step further created realistic synthetic observations of Dale et al. (2014) simulations at different distances, angles and time-steps with the FLUXCOMPENSATOR. With this set of realistic synthetic observations we tested the accuracy of techniques which are commonly used to estimate the SFR (Koepferl et al. 2016b and Koepferl et al., in prep.) and the gas mass, dust surface densities and dust temperatures (Koepferl et al. 2016a) of star-forming regions.

Already existing realistic synthetic observations of star-forming regions in SPITZER and HERSCHEL bands have been already published in several data releases: <https://doi.org/10.5281/zenodo.260106>, <https://doi.org/10.5281/zenodo.56424>, <https://doi.org/10.5281/zenodo.31293>, <https://doi.org/10.5281/zenodo.31294>.

5. FUTURE IMPLEMENTATIONS & SOFTWARE

With the FLUXCOMPENSATOR, as with HYPERION, we are still working on new tools to extend and improve the package in a continuous process. We are currently working on the following new applications of the FLUXCOMPENSATOR:

- Wavelength-dependent PSF convolution
- Noise standard deviation estimation directly from the information provided about the specific detector
- Saturation limits
- Gas radiative transfer post-processing
- Synthetic interferometry & line observations e.g. by building interfaces to the Common Astronomy Software Applications package (CASA)
- Astropy affiliated package

The FLUXCOMPENSATOR package has been designed to be able to post-process the radiative transfer output of HYPERION (Robitaille 2011) and is extendable to other radiative transfer codes. Further, this research made use

of Astropy, a community-developed core Python package for Astronomy (Astropy Collaboration et al. 2013), matplotlib, a Python plotting library (Hunter 2007), Pytest, test writing software for Python codes (Krekel et al. 2004–), Scipy, an open source scientific computing tool (Jones et al. 2001–), the NumPy package (van der Walt et al. 2011) and IPython, an interactive Python application (Pérez & Granger 2007).

6. SUMMARY

We have presented the FLUXCOMPENSATOR tool which can compute realistic synthetic observations from ideal radiative transfer observations, accounting for pixel resolution, reddening, PSF and filter convolution and noise. Taking into account these effects is important when modeling distant astronomical objects such as YSOs, star-forming regions or galaxies, where for instance multiple objects can be blended into a single source.

The FLUXCOMPENSATOR can be used to gauge and construct observational techniques, which extract properties of the observed objects or classify them. In Koepferl et al. (2015), Koepferl et al. (2016c), we use the FLUXCOMPENSATOR to produce realistic synthetic observations to test estimates of SFRs and gas and dust gas properties in star-forming regions in Koepferl et al. (2016a,b) and Koepferl et al., (in prep.).

The tool is now publicly available. For more information visit the FLUXCOMPENSATOR webpage <https://github.com/koepferl/FluxCompensator>, <https://doi.org/10.5281/zenodo.815629> and <http://FluxCompensator.readthedocs.io>.

7. ACKNOWLEDGEMENTS

We thank the referee for a constructive report that helped us improve the clarity and the strength of the results presented in our paper. This work was carried out in the Max Planck Research Group *Star formation throughout the Milky Way Galaxy* at the Max Planck Institute for Astronomy. C.K. is a fellow of the International Max Planck Research School for Astronomy and Cosmic Physics (IMPRS) at the University of Heidelberg, Germany and acknowledges support. C.K. also acknowledges support from the and the Bayerischen Gleichstellungsförderung. We would like to thank Jim Dale and Steffi Walch for the provided simulations.

REFERENCES

- Astropy Collaboration, Robitaille, T. P., Tollerud, E. J., et al. 2013, *A&A*, 558, A33
- Beaumont, C. N., Goodman, A. A., Kendrew, S., Williams, J. P., & Simpson, R. 2014, *ApJS*, 214, 3
- Brinch, C., & Hogerheijde, M. R. 2010, *A&A*, 523, A25
- Bronstein, I. N., Semendjajew, K. A., Musiol, G., & Mühlig, H. 2005, *Taschenbuch der Mathematik*, 6th edn. (Verlag Harri Deutsch)
- Carroll, B. W., & Ostlie, D. A. 1996, *An Introduction to Modern Astrophysics*, 1st edn. (Addison Wesley Publishing Company)
- . 2014, *An Introduction to Modern Astrophysics*, 2nd edn. (Pearson Education Limited)
- Cohen, M., Wheaton, W. A., & Megeath, S. T. 2003, *AJ*, 126, 1090
- Dale, J. E., Ercolano, B., & Bonnell, I. A. 2012, *MNRAS*, 424, 377
- Dale, J. E., Ngoumou, J., Ercolano, B., & Bonnell, I. A. 2014, *MNRAS*, 442, 694
- Dullemond, C. P., & Dominik, C. 2004, *A&A*, 417, 159
- Ercolano, B., Barlow, M. J., & Storey, P. J. 2005, *MNRAS*, 362, 1038
- Ercolano, B., Barlow, M. J., Storey, P. J., & Liu, X.-W. 2003, *MNRAS*, 340, 1136
- Ercolano, B., Koepferl, C., Owen, J., & Robitaille, T. 2015, *MNRAS*, 452, 3689
- Ercolano, B., Young, P. R., Drake, J. J., & Raymond, J. C. 2008, *ApJS*, 175, 534
- Feynman, R. P. 1977, *Feynman lectures on physics - Volume 1*, 6th edn. (Addison-Wesley)
- Girichidis, P., Walch, S., Naab, T., et al. 2016, *MNRAS*, 456, 3432
- Harries, T. J. 2000, *MNRAS*, 315, 722
- Hora, J. L., Carey, S., Surace, J., et al. 2008, *PASP*, 120, 1233
- Howell, S. B. 2006, *Handbook of CCD Astronomy*, 2nd edn.
- Hunter, J. D. 2007, *Computing In Science & Engineering*, 9, 90
- Jarrett, T. H., Cohen, M., Masci, F., et al. 2011, *ApJ*, 735, 112
- Jones, E., Oliphant, T., Peterson, P., et al. 2001–, *SciPy: Open source scientific tools for Python*, [Online; accessed 2012-2015]

- Kendrew, S., Simpson, R., Bressert, E., et al. 2012, *ApJ*, 755, 71
- Kendrew, S., Beuther, H., Simpson, R., et al. 2016, *ApJ*, 825, 142
- Kerton, C. R., Wolf-Chase, G., Arvidsson, K., Lintott, C. J., & Simpson, R. J. 2015, *ApJ*, 799, 153
- Kim, S.-H., Martin, P. G., & Hendry, P. D. 1994, *ApJ*, 422, 164
- Koepferl, C. M., Robitaille, T. P., & Dale, J. E. 2016a, *ArXiv e-prints*, arXiv:1606.08435
- . 2016b, *ArXiv e-prints*, arXiv:1606.08845
- Koepferl, C. M., Robitaille, T. P., Dale, J. E., & Biscani, F. 2016c, *ArXiv e-prints*, arXiv:1603.02270
- Koepferl, C. M., Robitaille, T. P., Morales, E., & Dale, J. E. (in preparation)
- Koepferl, C. M., Robitaille, T. P., Morales, E. F. E., & Johnston, K. G. 2015, *ApJ*, 799, 53
- Krekel, H., et al. 2004—, *pytest: helps you write better programs*, [Online; accessed 2012-2017]
- Molinari, S., Swinyard, B., Bally, J., et al. 2010, *PASP*, 122, 314
- Pérez, F., & Granger, B. 2007, *Computing in Science Engineering*, 9, 21
- Press, W. H., Teukolsky, S. A., Vetterling, W. T., & Flannery, B. P. 1992, *Numerical Recipes in FORTRAN. The Art of Scientific Computing*, 2nd edn. (Cambridge University Press)
- Quijada, M. A., Marx, C. T., Arendt, R. G., & Moseley, S. H. 2004, in *SPIE Conference Series*, Vol. 5487, SPIE Conference Series, ed. J. C. Mather, 244–252
- Reach, W. T., Megeath, S. T., Cohen, M., et al. 2005, *PASP*, 117, 978
- Robin, A. C., Reylé, C., Derrière, S., & Picaud, S. 2003, *A&A*, 409, 523
- Robitaille, T. P. 2011, *A&A*, 536, A79
- Robitaille, T. P., Whitney, B. A., Indebetouw, R., & Wood, K. 2007, *ApJS*, 169, 328
- Roccatagliata, V., Dale, J. E., Ratzka, T., et al. 2015, *A&A*, 584, A119
- Simpson, R. J., Povich, M. S., Kendrew, S., et al. 2012, *MNRAS*, 424, 2442
- Steinacker, J., Baes, M., & Gordon, K. D. 2013, *ARA&A*, 51, 63
- van der Walt, S., Colbert, S., & Varoquaux, G. 2011, *Computing in Science Engineering*, 13, 22
- Walch, S., Girichidis, P., Naab, T., et al. 2015, *MNRAS*, 454, 238
- Wright, E. L., Eisenhardt, P. R. M., Mainzer, A. K., et al. 2010, *AJ*, 140, 1868
- Yusef-Zadeh, F., Hewitt, J. W., Arendt, R. G., et al. 2009, *ApJ*, 702, 178

APPENDIX
DATABASE OVERVIEW

Here we provide the information, which the FLUXCOMPENSATOR includes in the built-in database. The corresponding references are given in the footnotes.

TABLE 2
INFORMATION ABOUT TELESCOPES AND DETECTORS PROVIDED IN THE FLUXCOMPENSATOR DATABASE

telescope name	diameter [cm]	detector		origin	filter wavelength [μ m]			α	β	built-in	PSF ^a resolution [$\frac{\text{arcsec}}{\text{pixel}}$]	sampled
		name	zero-point [Jy]		center	min	max					
2MASS	130. ^b	J[1.2]	1594. ^{cd}	cd	1.235 ^{cd}	1.062 ^c	1.450 ^c	1	0	-	-	-
2MASS	130. ^b	H[1.7]	1024. ^{cd}	cd	1.662 ^{cd}	1.289 ^c	1.914 ^c	1	0	-	-	-
2MASS	130. ^b	K[2.2]	666.7 ^{cd}	cd	2.159 ^{cd}	1.900 ^c	2.399 ^c	1	0	-	-	-
SPITZER	85. ^e	IRAC[3.5]	280.9 ^{fg}	hi	3.550 ^j	3.081 ^h	4.010 ^h	1 ^{gk}	0 ^{gk}	x	1.221	4
SPITZER	85. ^e	IRAC[4.5]	179.7 ^{fg}	hi	4.493 ^j	3.722 ^h	5.222 ^h	1 ^{gk}	0 ^{gk}	x	1.213	4
SPITZER	85. ^e	IRAC[5.7]	115.0 ^{fg}	hi	5.731 ^j	4.744 ^h	6.623 ^h	1 ^{gk}	0 ^{gk}	x	1.222	4
SPITZER	85. ^e	IRAC[8]	64.9 ^f	hi	7.872 ^j	6.151 ^h	10.497 ^h	1 ^{gk}	0 ^{gk}	x	1.220	4
SPITZER	85. ^e	MIPS[24]	7.17 ^l	m	23.68 ^l	18.005 ^m	32.307 ^m	-2 ⁿ	-1	x	2.49	5
SPITZER	85. ^e	MIPS[70]	0.778 ^l	m	71.42 ^l	49.960 ^m	111.022 ^m	-2 ⁿ	-1	x	9.85	5
SPITZER	85. ^e	MIPS[160]	0.159 ^l	m	155.9 ^l	100.085 ^m	199.92 ^m	-2 ⁿ	-1	x	16.	5
IRAS	57. ^o	IRAS[12]	30.88 ^p	q	12. ^q	7.0 ^q	15.5 ^q	1 ^r	-1	-	-	-
IRAS	57. ^o	IRAS[27]	7.26 ^p	q	25. ^q	16.0 ^q	31.5 ^q	1 ^r	-1	-	-	-
IRAS	57. ^o	IRAS[60]	1.11 ^p	q	60. ^q	27.0 ^q	87.0 ^q	1 ^r	-1	-	-	-
IRAS	57. ^o	IRAS[100]	0.39 ^p	q	100. ^q	65.0 ^q	140.0 ^q	1 ^r	-1	-	-	-
HERSCHEL	350. ^s	PACS[70]	0.78 ^p	t	70. ^u	48.721 ^t	157.480 ^t	1 ^v	-1	x	4.	10
HERSCHEL	350. ^s	PACS[100]	0.38 ^p	t	100. ^u	48.960 ^t	186.916 ^t	1 ^v	-1	x	4.	10
HERSCHEL	350. ^s	PACS[160]	0.14 ^p	t	160. ^u	105.263 ^t	500.000 ^t	1 ^v	-1	x	4.	10
HERSCHEL	350. ^s	SPIRE[250]	0.06 ^p	w	250. ^s	115.015 ^w	291.411 ^w	1 ^x	-1	x	6.	10
HERSCHEL	350. ^s	SPIRE[350]	0.03 ^p	w	350. ^s	137.397 ^w	419.451 ^w	1 ^x	-1	x	6.	10
HERSCHEL	350. ^s	SPIRE[500]	0.01 ^p	w	500. ^s	316.429 ^w	603.042 ^w	1 ^x	-1	x	6.	10
WISE	40. ^y	WISE[3.4]	309.540 ^z	aabb	3.353 ^z	2.53 ^{bb}	6.50 ^{bb}	2 ^{cc}	0	-	-	-
WISE	40. ^y	WISE[4.6]	171.787 ^z	aabb	4.603 ^z	2.53 ^{bb}	8.00 ^{bb}	2 ^{cc}	0	-	-	-
WISE	40. ^y	WISE[12]	31.674 ^z	aabb	11.562 ^z	2.53 ^{bb}	28.55 ^{bb}	2 ^{cc}	0	-	-	-
WISE	40. ^y	WISE[22]	8.363 ^z	aabb	22.088 ^z	2.53 ^{bb}	28.55 ^{bb}	2 ^{cc}	0	-	-	-

^aPSFs origin: http://dirty.as.arizona.edu/~kgordon/mips/conv_psfs/conv_psfs.html

^b2MASS Handbook: http://www.ipac.caltech.edu/2mass/releases/first/doc/sec3_1a.html

^c2MASS Handbook: http://www.ipac.caltech.edu/2mass/releases/allsky/doc/sec6_4a.html

^dCohen et al. (2003)

^eSpitzer Handbook:

<http://irsa.ipac.caltech.edu/data/SPITZER/docs/spitzermission/missionoverview/spitzertelescopehandbook/13/>

^fIRAC Handbook: <http://irsa.ipac.caltech.edu/data/SPITZER/docs/irac/iracinstrumenthandbook/17/>

^gReach et al. (2005)

^hIRAC Handbook: <http://irsa.ipac.caltech.edu/data/SPITZER/docs/irac/calibrationfiles/spectralresponse/>

ⁱQuijada et al. (2004)

^jIRAC Handbook: <http://irsa.ipac.caltech.edu/data/SPITZER/docs/irac/iracinstrumenthandbook/18/>

^kHora et al. (2008)

^lMIPS Handbook: <http://irsa.ipac.caltech.edu/data/SPITZER/docs/mips/mipsinstrumenthandbook/49/>

^mMIPS Handbook: <http://irsa.ipac.caltech.edu/data/SPITZER/docs/mips/calibrationfiles/spectralresponse/>

ⁿMIPS Handbook: <http://irsa.ipac.caltech.edu/data/SPITZER/docs/mips/mipsinstrumenthandbook/51/>

^oIRAS Handbook: http://irsa.ipac.caltech.edu/IRASdocs/iras_mission.html

^pFilter information: <http://svo2.cab.inta-csic.es/theory/fps/index.php>

^qIRAS Handbook: <http://irsa.ipac.caltech.edu/IRASdocs/exp.sup/ch2/tabC5.html>

^rIRAS Handbook: <http://lambda.gsfc.nasa.gov/product/iras/docs/exp.sup/ch6/C3.html>

^sHerschel Handbook: <http://herschel.esac.esa.int/Docs/SPIRE/html/>

^tPACS Handbook: <https://nhscsci.ipac.caltech.edu/sc/index.php/Pacs/FilterCurves>

^uPACS Handbook: <http://herschel.esac.esa.int/Docs/PACS/html/ch03s02.html>

^vPACS Handbook: <http://herschel.esac.esa.int/Docs/PACS/html/ch03s03.html>

^wprovided by the *Herschel* helpdesk

^xSPIRE Handbook: http://herschel.esac.esa.int/hcss-doc-11.0/load/spire_drg/html/ch05s07.html

^yWISE Handbook: http://wise2.ipac.caltech.edu/docs/release/allsky/expsup/sec3_2.html

^zJarrett et al. (2011)

^{aa}Wright et al. (2010)

^{bb}WISE Handbook: http://wise2.ipac.caltech.edu/docs/release/prelim/expsup/sec4_3g.html

^{cc}WISE Handbook: http://wise2.ipac.caltech.edu/docs/release/allsky/expsup/sec4_4h.html